

Correspondent: Samuel C. C. Ting

Department of Physics, M.I.T.

617-864-6900-X 5822

PROPOSAL TO STUDY ELECTROPRODUCTION WITH COINCIDENCE

TECHNIQUES AT HIGH ENERGIES

E. Bird, C. Halliwell, R. Morrison, John Walters

Department of Physics, Carleton University, Ottawa

and

J. D. Prentice,

Department of Physics, University of Toronto, Toronto

and

E. Coleman, T. Fesesse, Y. Makdisi

Department of Physics, University of Minnesota

and

U. J. Becker, P. J. Biggs, W. Busza, M. Chen, T. Nash

H. F. W. Sadrozinski, Samuel C. C. Ting, Sau Lan Wu

Department of Physics and Laboratory for Nuclear Science,

Massachusetts Institute of Technology

## ABSTRACT

Using the large aperture spectrometer of proposal 144 and the electron beam with the tagging system removed we propose to study deep inelastic electron scattering at incident electron energies between 50 and 150 GeV, for values of  $q^2$  between 1 and 20  $\text{GeV}^2/c^2$  and  $\nu$  between 10 and 130 GeV. The spectrometer will detect not only the scattered electron but also most of the secondary particles.

### Introduction

We propose to study electroproduction at energies up to 150 GeV using the same apparatus and beam (without the tagging system) proposed by our group for a study of photoproduction (NAL 144).

The motivation for this type of experiment has been so thoroughly discussed in the literature and in NAL proposals for deep inelastic  $\mu p$  scattering that we will simply outline the most important results that can be expected for this experiment: (Throughout we shall use standard notations and definitions.)<sup>1</sup>

(a) A detailed study of the inelastic form factor

$W_2(q^2, \nu)$  over a wide range of  $q^2$  (1 to 20  $\text{GeV}^2/c^2$ ),  
and  $\nu$  (10 to 130 GeV).

$W_2$  is defined through the following differential cross-section for inelastic hadronic electroproduction.

For small angles, 
$$\frac{d^2\sigma}{dq^2 d\nu} \simeq \frac{4\pi\alpha^2}{q^4} \frac{E'}{E} W_2(q^2, \nu) \dots (1)$$

- (b) The multiplicity and spectra of  $\pi^{\pm}$  in electroproduction as a function of  $q^2$  and  $\lambda$  (over the same range as above).
- (c) Check of  $\mu$ -e universality by comparing the results of this experiment with the  $\mu p$  experiments at NAL.
- (d) Search for the Lee-Wick high mass photon which would modify the photon propagator and so give a deviation from the scaling prediction.

It is possible in the future that two other experiments of interest can successfully be done with this apparatus. They are measurements of wide angle bremsstrahlung (QED test) and the  $q^2$  dependence of  $\rho$  electroproduction.

Use of the photon beam without the tagging radiator provides us with an electron beam well matched to the requirements of this experiment. Intensities of  $>10^7$   $e^-$ /pulse should be available with this beam at the required purity. As a result, the expected rates for this experiment compare favourably with the large scale  $\mu p$  experiment now being constructed for NAL.

In page 8 we will outline the rates expected as a function of  $\lambda$  and  $q^2$  at 150 GeV incident energy. From these calculations we can determine a reasonable bin size so that the statistical error in the measured cross section will approximately equal the amount by which the cross section varies across the bin. When this condition is satisfied, systematic errors caused by

Monte Carlo estimates of the proper weighted center of the bin are minimized. The bin size determines the resolution that is required in the experiment. Using rates in a typical region near the center of the  $(\nu, q^2)$  acceptance (at  $\nu \approx 70$  GeV,  $q^2 \approx 10 (\text{GeV}/c)^2$ ) and requiring about the same number of  $\nu$  and  $q^2$  bins, we find that a reasonable bin size is  $\Delta\nu = 5$  GeV and  $\Delta q^2 = 1 (\text{GeV}/c)^2$ . Rates in a typical bin will have a statistical error of  $\sim 5$  % after 400 hours of running.

The electron beam:

To meet the requirements stated above, two modifications to the beam<sup>2</sup> are necessary. First, the beam must be more strongly collimated at the first focus to reduce the momentum acceptance to  $\pm 1$  %. This results in a loss of about 30 % in intensity. Second, using the asymmetric shape of the beam and hodoscopes at the exit of the last magnet and just before the target, the incident  $e^-$  angle will be measured to  $\pm 0.2$  mrad.

Spectrometer

A slightly modified version of the forward spectrometer described in proposal No. 144 can be used for this experiment. See diagram 1. The spectrometer can be separated into two parts as described in proposal 144.

- a) A small solid angle focusing spectrometer consists of two magnets (M1 and M2) and four sets of chambers and counters. The angular acceptance is

$$|\theta_x| < 10 \text{ mrad}$$
$$10 < |\theta_y| < 31 \text{ mrad}$$

The essential modification to the spectrometer is a 150 radiation length Heavimet beam stopper (approximately 13 cm high x 16 cm wide x 50 cm long) which will be inserted directly in front of the first magnet to stop the primary electron beam. It subtends an angle of  $\pm 10$  mrad at the target in the vertical direction and  $\pm 12$  mrad in the horizontal. As in P-144 wire chambers will be positioned at A, B, C and D to measure the angles and momenta of the scattered electron and other associated charged particles.

The angle of the scattered electron in the vertical (bending) plane  $\theta_y$ , is measured at D since particles with the same production angle but different momenta will be focussed there. The angle in the non-bending

plane,  $\theta_x$ , is defined by all four planes of wire chambers.

The accuracy of the  $\theta_y$  measurements is  $\ll \pm 0.1$  mrad.

The accuracy in  $\theta_x$  is  $\ll \pm 0.04$  mrad.

The momentum of the scattered electron is determined to an accuracy of  $\pm 0.015$  p (%), where p is in GeV/c.

- b) A large solid angle spectrometer consisting of one magnet and two sets of chambers and counters A and B.

The angular acceptance is

$$|\theta_x| < 94 \text{ mrad}$$

$$|\theta_y| < 31 \text{ mrad}$$

The events detected by the large angle acceptance spectrometer can be further separated into two classes:

- (i) There is at least one particle detected by the small angle spectrometer as well. In this case the interacting point inside the target can be located to better than  $\pm 2$  mm and therefore the scattered angle of the electron can be determined to  $\sim \pm 0.3$  mr.
- (ii) There is no particle detected by the small angle spectrometer. In this case, the interacting point inside the target is known only to the extent of the width of the beam in the bending plane, i. e.  $\sim \pm 5$  mm. Therefore

the scattered angle of the electron is determined to  
 $\sim \pm 0.7$  mr.

### Target

The length of the hydrogen target is limited by the magnitude of the bremsstrahlung corrections. In general we require the contributions of the external bremsstrahlung to be less than the contributions of the internal bremsstrahlung. Details of the calculations of real bremsstrahlung and internal radiative corrections to deep inelastic electroproduction can be found in the literature.<sup>3</sup> From these calculations we find that, in our range of  $q^2$  ( $1 < q^2 < 20(\text{GeV}/c)^2$ ), the correction due to internal radiative effects is equivalent to the real bremsstrahlung in a hydrogen target of between 40 and 50 cms. For that reason we have decided to use a length of 25 cm. We assume this target length in all subsequent rate estimates.

### Intensity and Pion Contamination of the Beam

We will know the  $e^-$  intensity and  $\pi^-/e$  ratio for the beam precisely well before this experiment is running. At this time we can only use estimates based on calculations made when the beam was designed.<sup>2</sup>

To obtain the lowest  $\pi^-/e$  ratio that is consistent with the intensity requirements of the experiment, we use an incident proton angle of 2 mrad. At 150 GeV, the number of  $e^-$ /pulse ( $10^{13}$  500 GeV p) is  $5 \times 10^7$  and the

$\pi^-/e$  ratio is  $2 \times 10^{-4}$ . By using U as a radiator instead of Pb we multiply the  $\pi^-/e$  ratio by 0.88. Reducing the thickness of the radiator from 0.5 r<sub>l</sub> to 0.3 r<sub>l</sub> the  $\pi^-/e$  ratio is improved by a factor of 0.67 with a loss of 1/3 of the  $e^-$ . Using a longer primary Be target we can filter more  $\pi^-$  and obtain a 25 % reduction of  $\pi^-/e$  ratio with only a 30 % reduction in  $e^-$  intensity. The rates so far assume collimation at the first focus to eliminate the halo in the vertical (non-bending) plane). In the bending plane there is dispersion at the first focus so that collimation helps very little. However, in the region before the experimental target dispersion is cancelled and collimation of the halo will reduce the  $\pi^-/e$  ratio by 1/3 with almost no loss of  $e^-$ . Taking advantage of all these factors we can reduce the  $\pi^-/e$  ratio to  $3 \times 10^{-5}$  with an  $e^-$  intensity of  $2.5 \times 10^7 e^-/\text{pulse}$ .

### $\pi^-/e$ Discrimination

Using a technique similar to that employed by the SLAC/MIT group<sup>4</sup> (i. e.  $\frac{dE}{dx}$  counters behind 1 radiation length of lead, followed by total absorption shower counter) there should be no difficulty in obtaining a rejection ratio between  $10^{-3}$  and  $10^{-4}$  for pions as compared with electrons. If necessary, this rejection ratio could further be increased by observing the shower built up in a sandwich of a few Pb plates and proportional chambers.



Negative charged pions can be produced either from an incident electron or from an incident pion. Background due to the former is negligible since it is reduced by  $10^{-3}$  to  $10^{-4}$  by the detector. Background from pion induced events is more serious since the cross section is  $10^5$  to  $10^6$  higher than that due to the deep inelastic electron cross section for some values of  $q^2$  and  $\nu$ . As discussed earlier we expect that the ratio of  $\pi^-$  over  $e^-$  in the beam will be  $3 \times 10^{-5}$ . Using the detector rejection of  $10^3$  we find that the  $\pi^-$  induced events will contribute a background of less than 3 %, which is tolerable.

#### Event rates:

Using Eq. (1) we have calculated the data rate for deep inelastic ep scattering events as a function of  $q^2$  and  $\nu$ . The event rates per bin of  $\Delta q^2 = 1 (\text{GeV}/c)^2$  and  $\Delta \nu = 5 \text{ GeV}$  are calculated with  $2.5 \times 10^7 e^-/\text{pulse}$  at an incident energy of 150 GeV on a 25 cm liquid hydrogen target and 400 hours of running. Four contours of constant rates are shown in Fig 2, from these we see that it is possible to obtain a sizeable number of events up to  $q^2 \approx 25 (\text{GeV}/c)^2$  for  $\nu \approx 30 \text{ GeV}$  and  $q^2 \approx 12 (\text{GeV}/c)^2$  for  $\nu \approx 100 \text{ GeV}$ . This will cover  $\omega$  up to  $\approx 50$  and  $W$  up to  $\approx 16 \text{ GeV}$ . Simulated results are shown in figure 3.

#### Background due to knock-on electrons:

The dominating background in our case is due to knock on electrons from ee scattering, which have a momentum

distribution<sup>5</sup>

$$\frac{d\sigma}{dE} = 2\pi r_e^2 \frac{m_e}{(E')^2}$$

where  $r_e$  is the classical radius of the electron. The knock on electrons are strongly peaked at low energy, therefore most of them are swept away by the first magnet (M1) of the spectrometer. We shall set a cut-off energy for the scattered electron by requiring that at least one shower counter gives a signal greater than that due to a 20 GeV  $e^-$  shower in order to trigger the system. Very few triggers/pulse will then result from knock on electrons. These events can be rejected off line since they contain no particles other than the electrons. Since the multiplicity at such high energy is very high, one alternative scheme for the trigger system is to require the presence of at least one charged particle in addition to the scattered electron.

Beam requirements: 700 hrs of  $10^{13}$  protons/pulse at 500 GeV:

this will be subdivided into

400 hrs of 150 GeV  $e^-$  beam energy

160 hrs of 100 GeV  $e^-$  beam energy

140 hrs of 50 GeV  $e^-$  beam energy

## References

1. G. Miller et al Phys. Rev. D5, 528, 1972
2. C. Halliwell et al Nucl. Instr. & Meth. in press 1972
3. L. W. Mo and Y. S. Tsai Rev. Mod. Phys. 41, 205, 1969
4. M. Breidenbach, Ph. D. Thesis M.I.T. 1970
5. Mott & Massey, The theory of Atomic Collisions, 3rd Ed., 1965 p 818

## Figure Captions

1. Spectrometer configuration for deeply inelastic electron scattering. A and C are wire proportional chambers, B and D are combinations of converter material,  $dE/dX$  counters, total absorption counters and wire proportional chambers. See P-144 for details.
2. Rates expected as a function of  $\nu, \xi^2$ . Curves are lines of constant rate. Boxes show bin size and rate expected in bin along the line.
3. Example of statistics that will be obtained in measurement of  $\nu W_2$  as a function of  $q^2$  and  $\xi^2$  after 400 hours running at 150 GeV  $e^-$  energy.

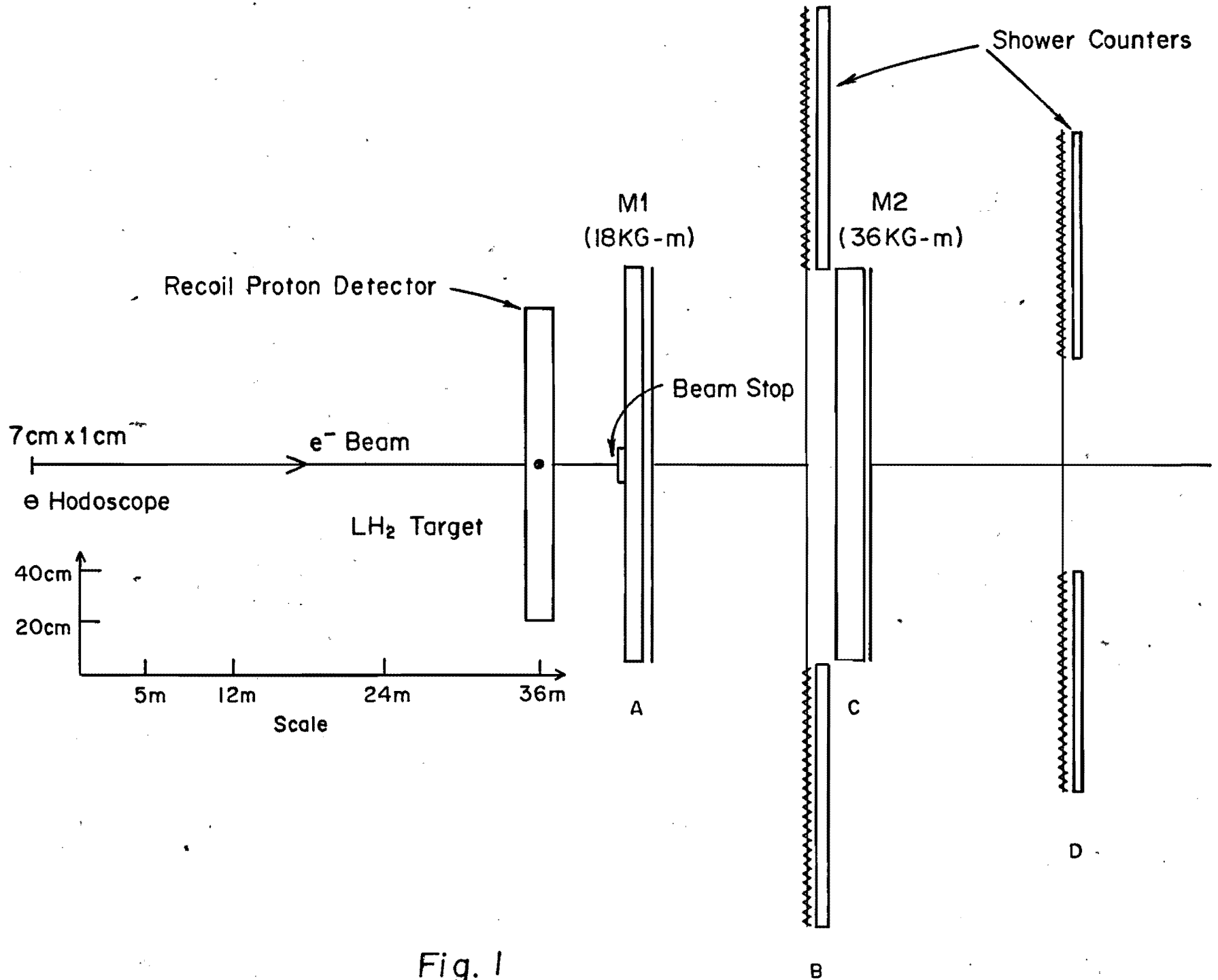
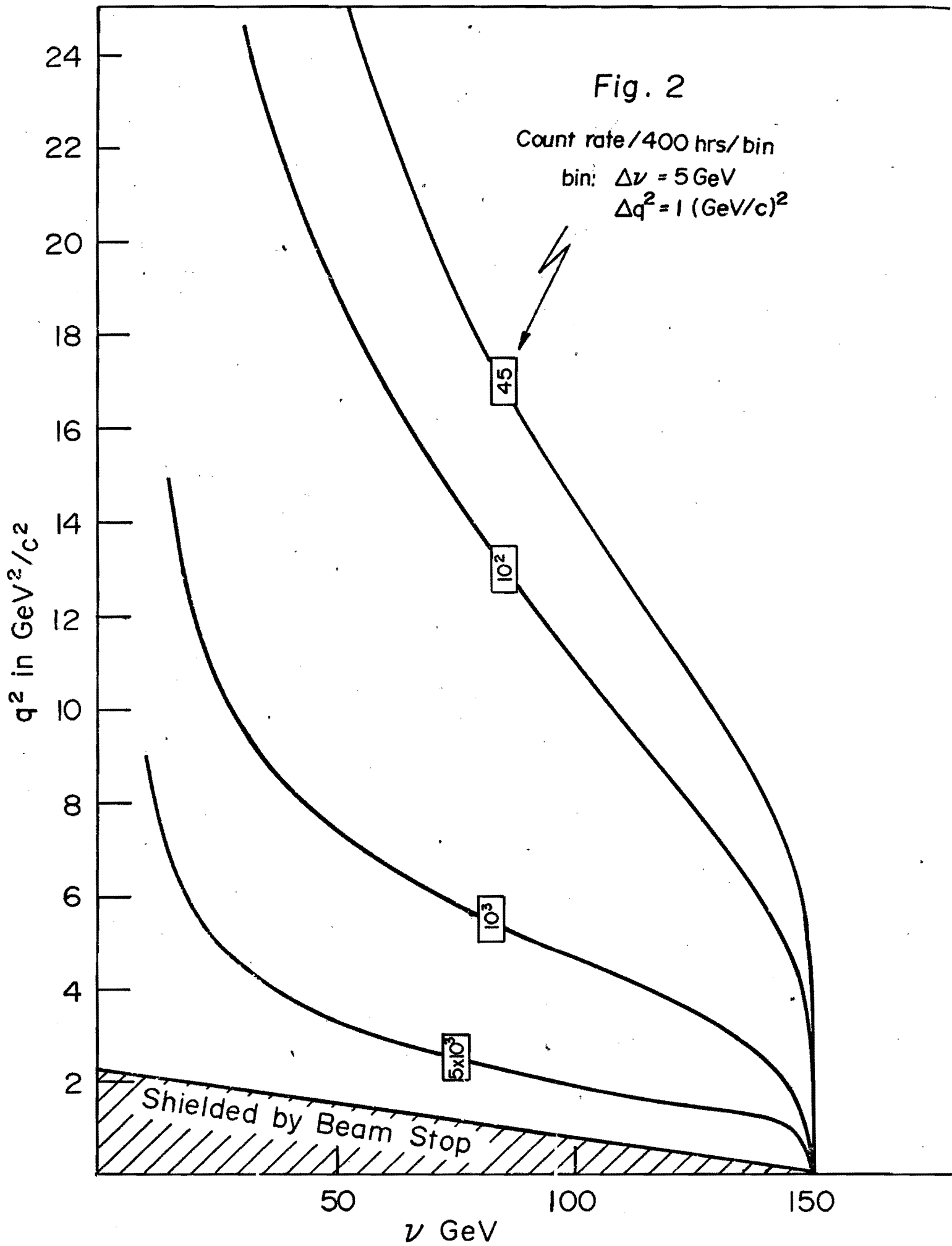


Fig. 1



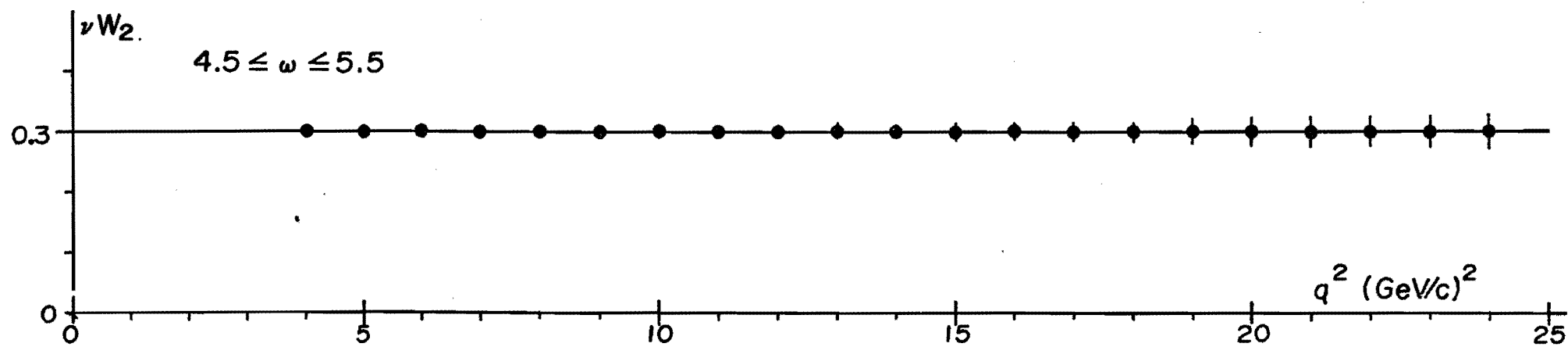
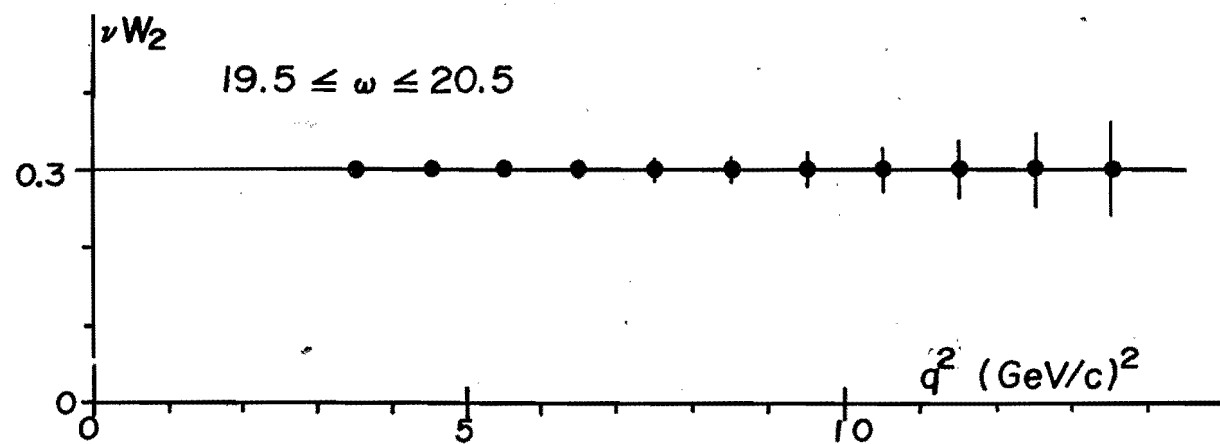
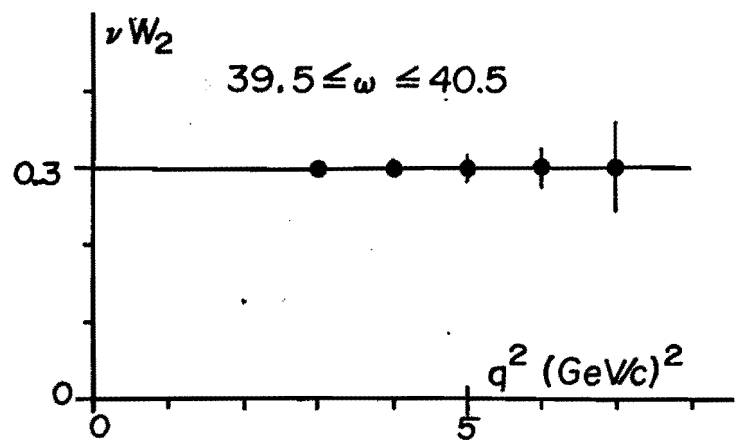


Fig. 3

Addendum to 174.

In the original 174 we assumed a 500 BeV/c  $10^{13}$  proton/pulse beam and two large new magnets used in NAL 144. That proposal is now inoperative.

After consultation with NAL staff we submit this realistic addendum to do electron physics at 40 - 120 GeV/c region ( $q^2 = 1-20 \text{ GeV}^2/c$ ) with:

1. 400 BeV,  $10^{13}$  protons/pulse proton beam;
2. two existing CEA magnets, which have been committed to us: Henry Higgins (6.22' x 33.84" x 15") and Jolly Green Giant (7.2' x 59" x 15");
3. proportional chambers, PDP11/45, fast electronics, etc. from our current BNL experiment - all will be available in 24 months' time;
4. the size and scope of this experiment can be accommodated at the end section of the two stage beam.

The physics of this experiment are the same as the original 174 - except scaling down from 500 BeV/protons to 400 BeV/c protons - will reduce the  $\nu$ ,  $q^2$  slightly.

In particular, the physics that can be done with this set up are:



- (a) A detailed study of the inelastic form factor  $W_2(q^2, \nu)$  over a wide range of  $q^2$  (1 to 20  $\text{GeV}^2/c^2$ ), and  $\nu$  (10 to 110 GeV).

$W_2$  is defined through the following differential cross-section for inelastic hadronic electroproduction.

For small angles,

$$\frac{d^2\sigma}{dq^2 d\nu} = \frac{4\pi\alpha^2}{q^4} \frac{E'}{E} W_2(q^2, \nu) \quad (1)$$

- (b) The multiplicity and spectra of  $\pi^\pm$  in electroproduction as a function of  $q^2$  and  $\nu$  (over the same range as above).
- (c) Check of  $\mu$ -e universality by comparing the results of this experiment with the  $\mu p$  experiments at NAL.
- (d) Search for the Lee-Wick high mass photon which would modify the photon propagator and so give a deviation from the scaling prediction.

It is possible in the future that two other experiments of interest can successfully be done with this apparatus. They are measurements of wide angle bremsstrahlung (QED test) and the  $q^2$  dependence of  $\beta$  electroproduction.

Use of the photon beam without the tagging radiator provides us with an electron beam well matched to the requirements of this experiment. Intensities of  $>10^7$   $e^-$ /pulse should be available with this beam at the required purity. As a result, the expected rates for this experiment compare favourably with the large scale

$\mu$ P experiment.

The electron beam, the H<sub>2</sub> target, the  $\pi/e$  discrimination, the bin size, the background due to knock on electrons, etc. have all been discussed in NAL 174.

We list briefly the property of the spectrometer and event rate for the set up.

### Spectrometer

The spectrometer is shown in diagram 1,2. The spectrometer can be separated into two parts:

- a) A small solid angle focusing spectrometer consists of two magnets (M1 and M2) and four sets of chambers and counters. The angular acceptance is

$$|\theta_x| < 14.4 \text{ mrad}$$

$$|\theta_y| < 57 \text{ mrad}$$

A 150 radiation length Heavimet beam stopper (approximately 13 cm high x 16 cm wide x 50 cm long) will be inserted directly in front of the first magnet to stop the primary electron beam. For the target position as shown in Figs. 1 and 2 it subtends an angle of  $\pm 20.4$  mrad at the target in the vertical direction and  $\pm 25$  mrad in the horizontal. In order to cover low  $q^2$  region, for about 10 % of the running time, the H<sub>2</sub> target has to be moved 2 m away from the detector. Wire chambers will be used to measure the angles and momenta of the scattered electron and other associated charged particles.

The angle of the scattered electron in the vertical (bending) plane  $\theta_y$ , is measured by the chambers at the far end (positions 6 and 7) since particles with the same production angle but different momenta will be focused there. The angle in the non-bending plane,  $\theta_x$ , is defined by at least four planes of wire chambers. The accuracy of the  $\theta_y$  measurements is  $\sim \pm 0.1$  mrad. The accuracy in  $\theta_x$  is  $\sim \pm 0.04$  mrad.

The momentum of the scattered electron is determined to an accuracy of  $\pm 0.03$  p (%), where p is in GeV/c.

- b) A large solid angle spectrometer consisting of one magnet and two sets of chambers and counters at 3 and 8.

The angular acceptance is

$$|\theta_y| < 103 \text{ mrad}$$

$$|\theta_x| < 46 \text{ mrad}$$

The events detected by the large angle acceptance spectrometer can be further separated into two classes:

- (i) There is at least one particle detected by the small angle spectrometer as well. In this case the interacting point inside the target can be located to better than  $\pm 2$  mm and therefore the scattered angle of the electron can be determined to  $\sim \pm 0.8$  mr.

(ii) There is no particle detected by the small angle spectrometer. In this case, the interacting point inside the target is known only to the extent of the width of the beam in the bending plane, i. e.  $\sim \pm 5$  mm. Therefore the scattered angle of the electron is determined to  $\sim \pm 1.4$  mr.

### Event rates

Using Eq. (1) we have calculated the data rate for deep inelastic ep scattering events as a function of  $q^2$  and  $\nu$ . The event rates per bin of  $\Delta q^2 = 1(\text{GeV}/c)^2$  and  $\Delta \nu = 5$  GeV are calculated with  $2.0 \times 10^7$   $e^-$ /pulse at an incident energy of 120 GeV on a 30 cm liquid hydrogen target and 400 hours of running. Three contours of constant rates are shown in Fig. 3. From these we see that it is possible to obtain a sizeable number of events up to  $q^2 \approx 20 (\text{GeV}/c)^2$  for  $\nu \approx 30$  GeV and  $q^2 \approx 8 (\text{GeV}/c)^2$  for  $\nu \approx 100$  GeV. This will cover  $\omega$  up to  $\approx 50$  and  $W$  up to  $\approx 16$  GeV. Simulated results are shown in figure 4. The test of scaling behaviour of the form factor  $\nu W_2$  will be very conclusive.

Beam requirements: 700 hrs. of  $10^{13}$  protons/pulse at 400 GeV:

this will be subdivided into

400 hrs. of 120 GeV  $e^-$  beam energy

160 hrs. of 80 GeV  $e^-$  beam energy

140 hrs. of 40 GeV  $e^-$  beam energy

## Figure Captions

- 1., 2. Spectrometer configuration for deeply inelastic electron scattering. 1 - 6 are wire proportional chambers, 7 and 8 are combinations of converter material,  $dE/dX$  counters, total absorption counters and spark chambers.
3. Rates expected as a function of  $\nu$ ,  $q^2$ . Curves are lines of constant rate. Boxes show bin size and rate expected in bin along the line. Dotted lines are with 500 GeV,  $10^{13}$  proton/pulse, 400 hours of running, at  $E_e = 150$  GeV (original NAL 174). Solid lines are with 400 GeV,  $10^{13}$  proton per pulse, 400 hours of running at  $E_e = 120$  GeV.
4. Example of statistics that will be obtained in measurement of  $\nu W_2$  as a function of  $q^2$  and  $\omega$  after 400 hours running at 120 GeV  $e^-$  energy.

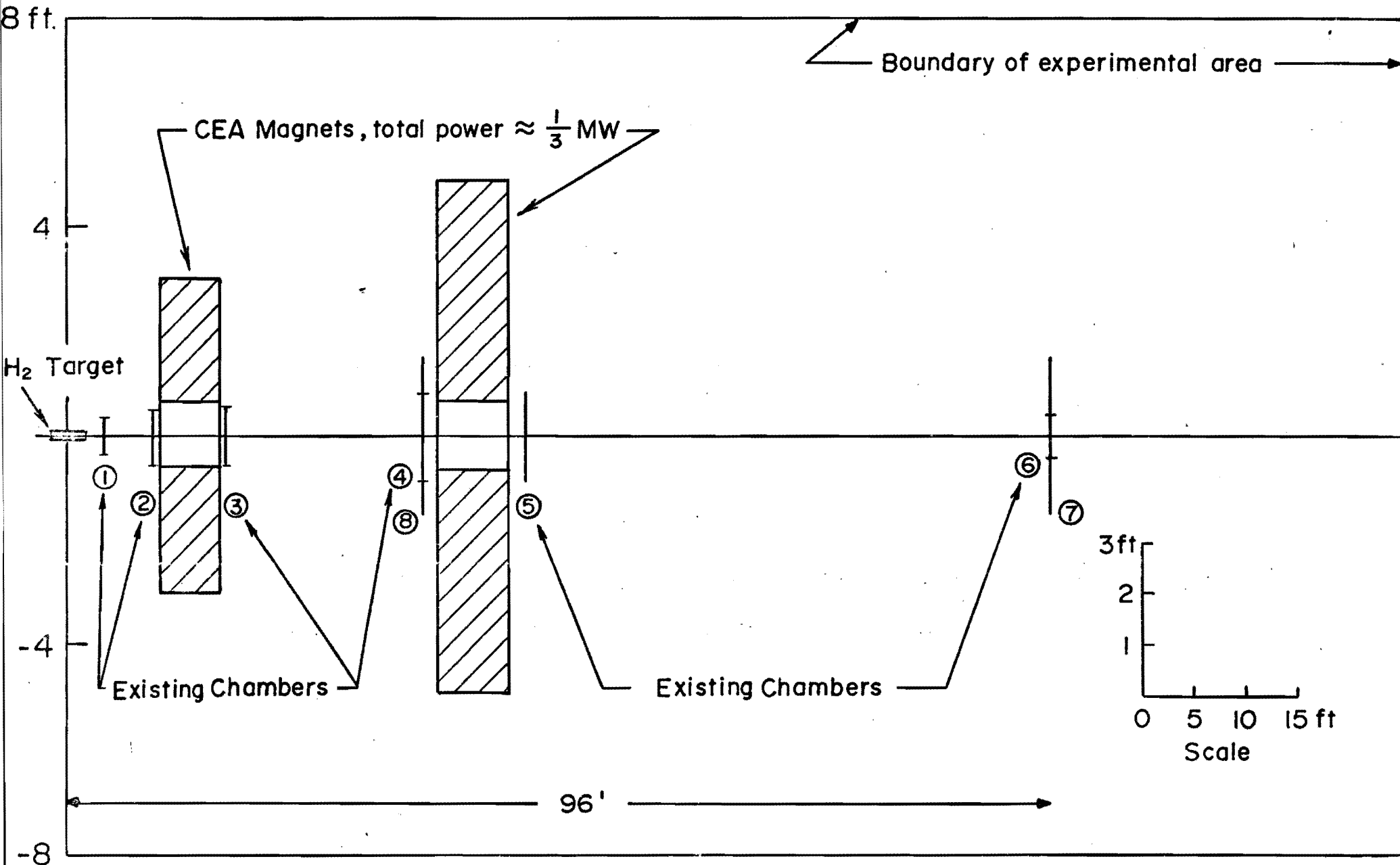


Fig.1. THE TOP VIEW OF THE SPECTROMETER

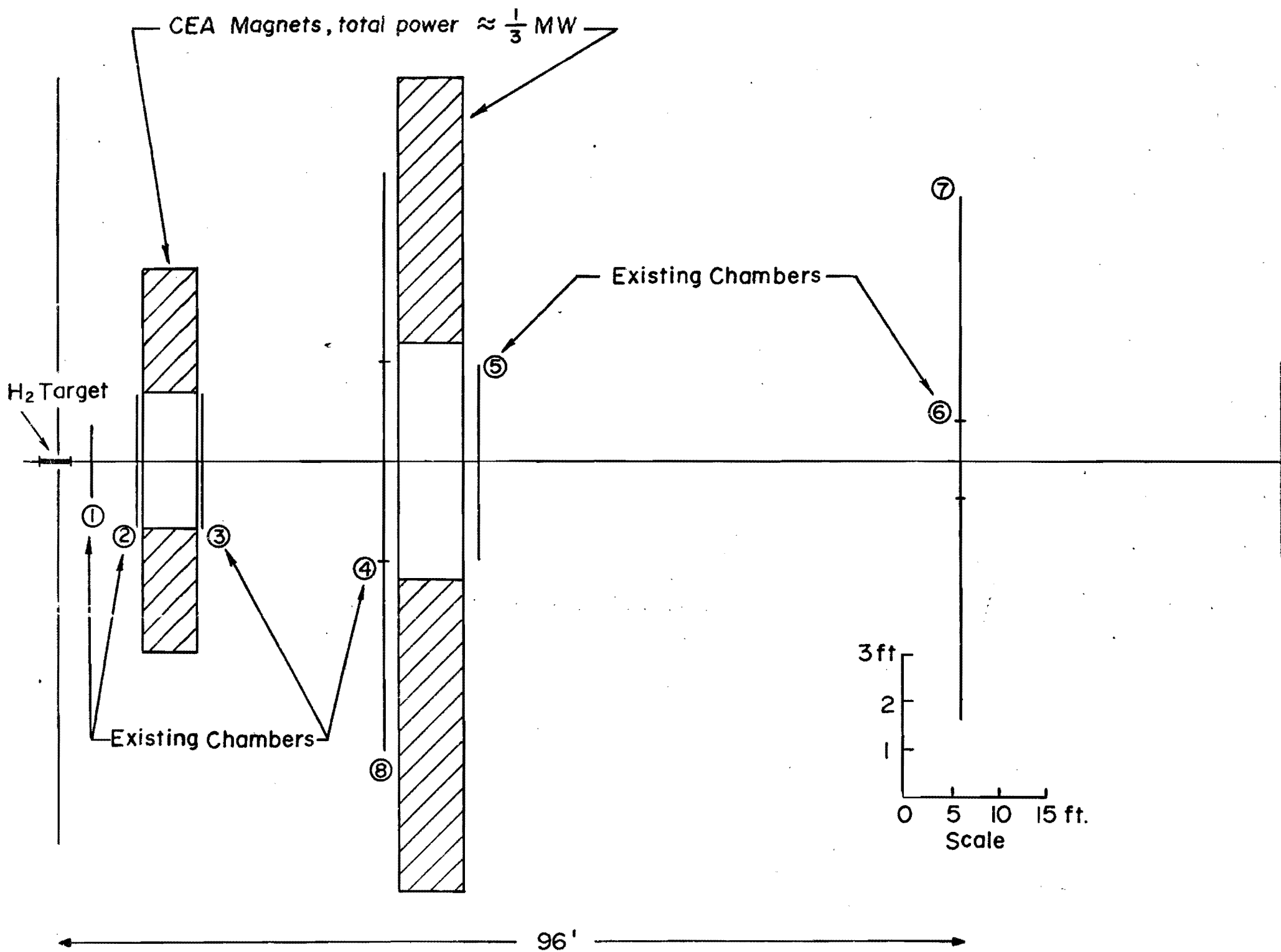


Fig. 2. THE SIDE VIEW OF THE SPECTROMETER

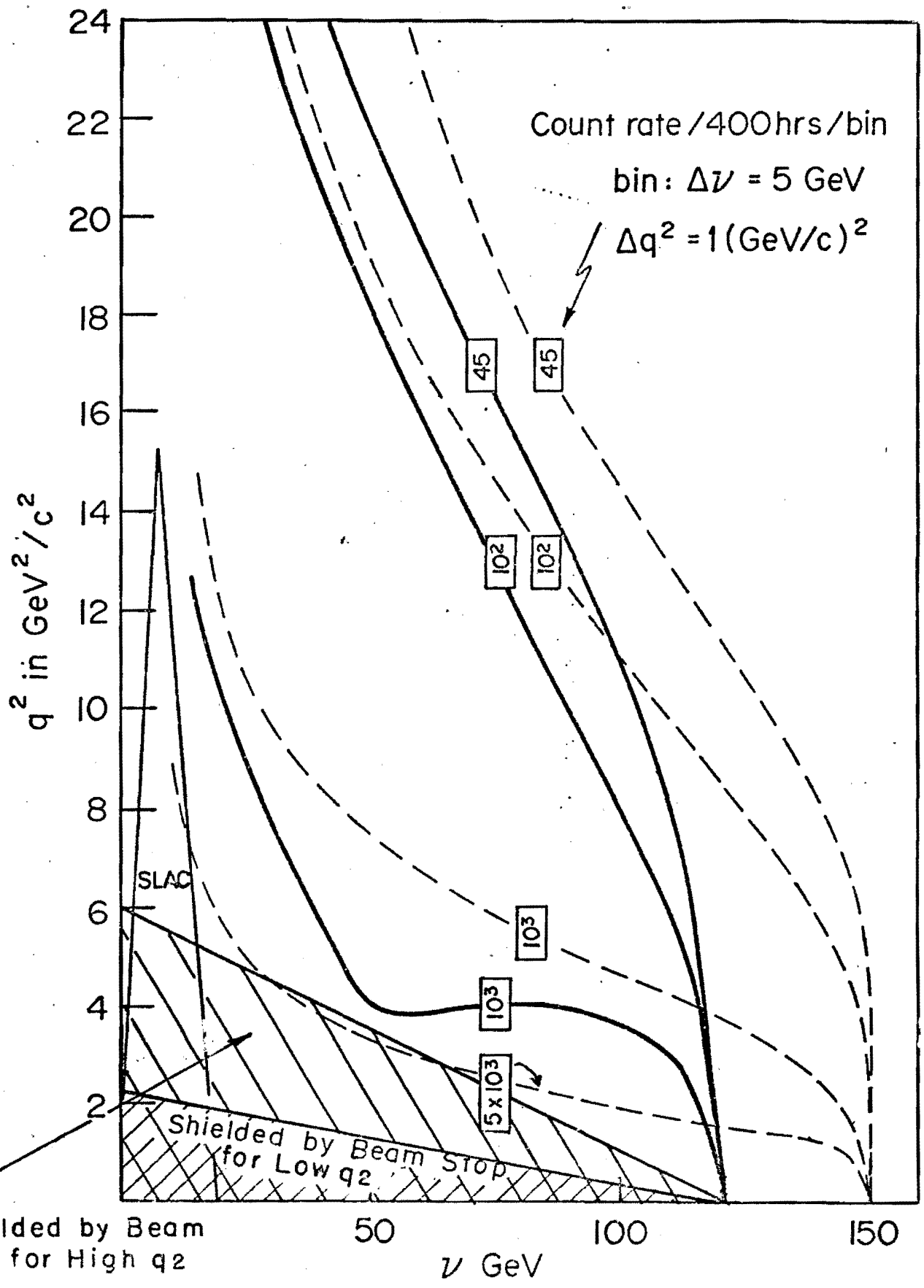


Fig. 3



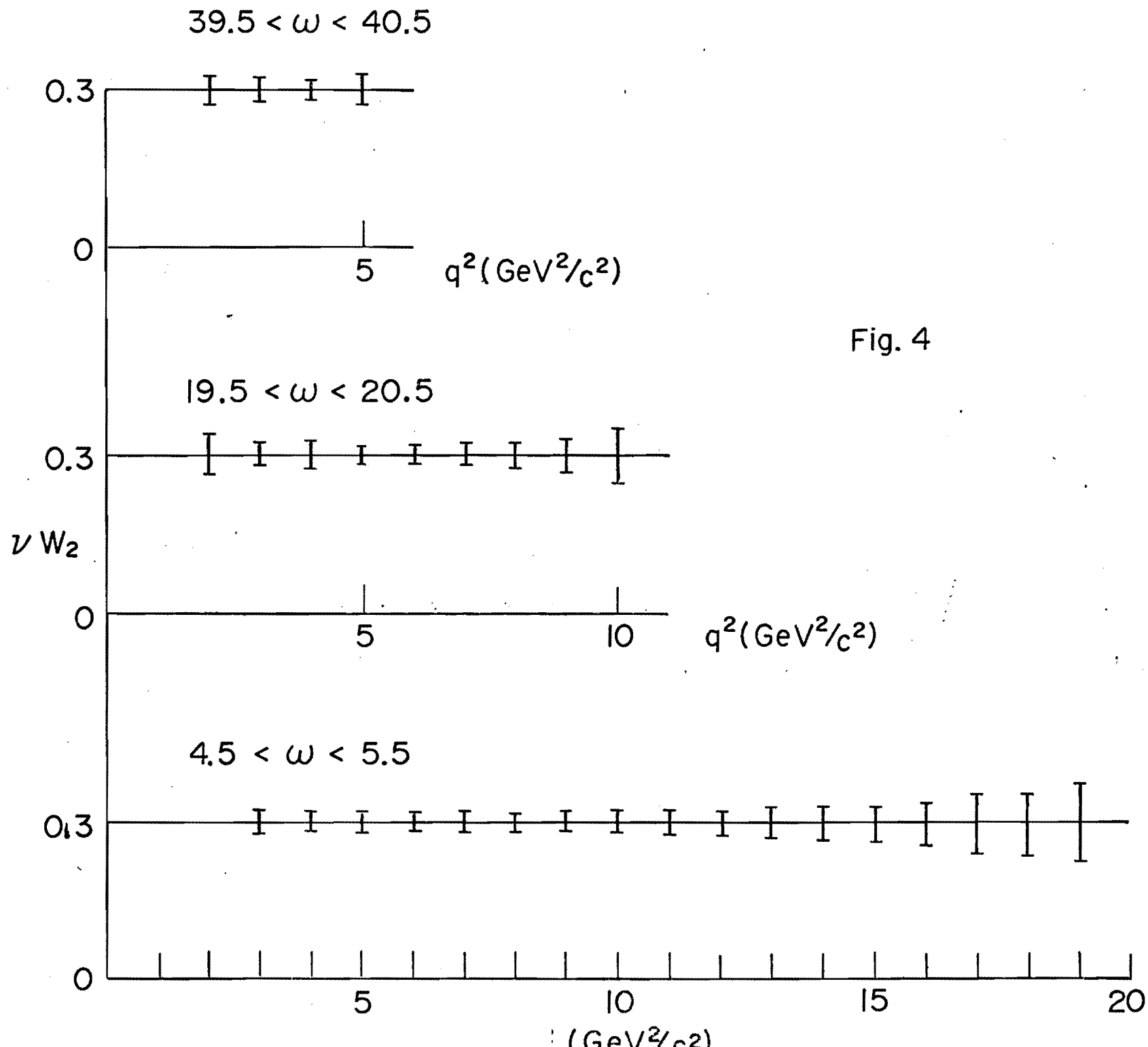


Fig. 4